

AG
T

*Algebraic & Geometric
Topology*

Volume 23 (2023)

**A mnemonic for the
Lipshitz–Ozsváth–Thurston correspondence**

ARTEM KOTELSKIY

LIAM WATSON

CLAUDIUS ZIBROWIUS



A mnemonic for the Lipshitz–Ozsváth–Thurston correspondence

ARTEM KOTELSKIY
LIAM WATSON
CLAUDIUS ZIBROWIUS

When \mathbb{k} is a field, type D structures over the algebra $\mathbb{k}[u, v]/(uv)$ are equivalent to immersed curves decorated with local systems in the twice-punctured disk. Consequently, knot Floer homology, as a type D structure over $\mathbb{k}[u, v]/(uv)$, can be viewed as a set of immersed curves. With this observation as a starting point, given a knot K in S^3 , we realize the immersed curve invariant $\widehat{HF}(S^3 \setminus \mathring{\nu}(K))$ of Hanselman, Rasmussen and Watson by converting the twice-punctured disk to a once-punctured torus via a handle attachment. This recovers a result of Lipshitz, Ozsváth and Thurston calculating the bordered invariant of $S^3 \setminus \mathring{\nu}(K)$ in terms of the knot Floer homology of K .

57K18, 57K31; 57R58

Recent work interprets relative versions of homological invariants in terms of immersed curves, including Heegaard Floer homology for manifolds with torus boundary (see Hanselman, Rasmussen and Watson [4]) as well as link Floer homology (see Zibrowius [23]), singular instanton knot homology (see Hedden, Herald and Kirk [7]), and Khovanov homology (see Kotelskiy, Watson and Zibrowius [12]) for 4-ended tangles. In particular, Section 5 of [12] classifies type D structures over a quiver algebra associated with a surface with boundary in terms of immersed curves on this surface; compare Haiden, Katzarkov and Kontsevich [2] and Hanselman, Rasmussen and Watson [4]. Denoting a field by \mathbb{k} , perhaps the simplest algebra to illustrate these classification results is $\mathcal{R} = \mathbb{k}[u, v]/(uv)$. This algebra arises as the path algebra of a quiver that is associated with the decorated surface shown in Figure 1. Work of Lekili and Polishchuk [13; 14] describes the role of \mathcal{R} , and its relationship with the twice-punctured disk, in the context of homological mirror symmetry; see in particular [14, Figures 1 and 2]. The algebra \mathcal{R} equipped with the Alexander and δ gradings $\text{gr}(u) = (-1, 1)$ and $\text{gr}(v) = (1, 1)$ plays a central role in knot Floer homology; see Dai, Hom, Stoffregen and Truong [1], for instance.

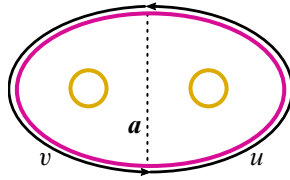


Figure 1: An arc system associated with the algebra \mathcal{R} .

Theorem 1 *Every bigraded type D structure over \mathcal{R} is equivalent to an immersed curve (decorated with local systems) in the twice-punctured disk, which is unique up to regular homotopy (and equivalence of local systems).*

As stated, this is a special case of a theorem proved in [12, Section 5] appealing to techniques from [4] (see also [23]). The observation could alternatively be extracted from [4, Section 3.4] (see the aside starting on page 2527 below accompanying Figure 8), and also follows from work of Haiden, Katzarkov and Kontsevich [2]; see Section 1.8 of [12] for more discussion. We will review the algebraic objects in Section 1 and, without reproducing the proof in full, explain some key steps in this special case in Section 2. Theorem 1 gives rise to a graphical interpretation γ for (a variant of) knot Floer homology ${}^{\mathcal{R}}CFK(Y, K)$, which is a bigraded type D structure over \mathcal{R} . Our proof is constructive and, in particular, foregrounds the role of vertically and horizontally simplified bases that arise in knot Floer homology. An explicit example of a curve γ in the twice-punctured disk is shown in Figure 2, left. This particular curve corresponds to the type D structure associated with the right-hand trefoil $T_{2,3}$ in S^3 :

$$[\diamond_1 \xleftarrow{u} \diamond_2 \xrightarrow{v} \diamond_3] = {}^{\mathcal{R}}CFK(S^3, T_{2,3}).$$

Note that, while the local system in this example is trivial, these are easy to add to the picture in general, being equivalent to isomorphism classes of flat vector bundles over the curves in question. There is an obvious handle attachment, identifying the two punctures in the disk, which yields a once-punctured torus. Denote this handle attachment by \frown and consider the curve $\frown(\gamma)$. Note that, given a choice of meridian on the torus, this operation has an inverse, which we will denote by \oslash .

Denote by $\widehat{HF}(M)$ the immersed curve in the once-punctured torus associated with a manifold M with torus boundary [4]. This is equivalent to the bordered Heegaard Floer invariant of M ; see Lipshitz, Ozsváth and Thurston [17]. Here is the mnemonic we propose:

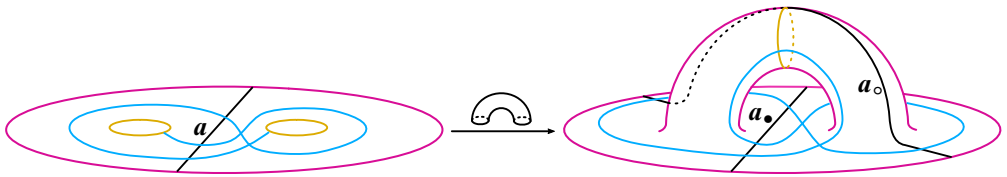


Figure 2: Adding a handle to the twice-punctured disk results in the once-punctured torus. This carries immersed curves to immersed curves; the immersed curve on the left corresponds to the type D structure ${}^{\mathcal{R}}CFK(S^3, T_{2,3}) = [\diamond_1 \xleftarrow{u} \diamond_2 \xrightarrow{v} \diamond_3]$, which is carried to the curve $\widehat{HF}(M)$, where M is the trefoil exterior $S^3 \setminus \mathring{\nu}(K)$.

Theorem 2 If γ is a curve representing the knot Floer invariant ${}^{\mathcal{R}}CFK(S^3, K)$ over the two-element field, then $\mathcal{C}(\gamma)$ is equivalent to $\widehat{HF}(M)$, where M is the exterior of the knot K . Conversely, given a meridian for $M = S^3 \setminus \mathring{\nu}(K)$, the curve $\mathcal{D}(\widehat{HF}(M))$ represents the knot Floer type D structure for K .

Figure 2 illustrates this theorem for the right-hand trefoil knot; the proof is given in Section 4.

Remark There is an apparent ambiguity in the statement of Theorem 2, namely the number of twists (along the belt of the handle \mathcal{C}) one adds to the noncompact component of the curve γ . However, recall that the curve $\widehat{HF}(M) \subset \partial M$ is null-homologous in M [4, Sections 5 and 6]; to resolve the ambiguity it is enough to identify the once-punctured torus obtained after adding the handle with the boundary of the knot exterior (minus a small disk). We identify the arc a_{\bullet} from Figure 2 with the meridian μ , and the second arc a_{\circ} with a longitude λ of K . This pair provides a bordered structure, in the sense of Lipshitz, Ozsváth and Thurston [17]. Concerning the framing λ : On one hand, there is a preferred choice given by the Seifert longitude λ_0 , and the corresponding identification is depicted in Figure 3, right. On the other hand, it is often easiest to work with the “blackboard framing”, which simply joins the endpoints of γ without new twisting as they run over the handle, as in Figure 2. In general, the latter gives the $2\tau(K)$ –framed longitude $\lambda_{2\tau} = 2\tau \cdot \mu + \lambda_0$, where the value $\tau(K)$ is the Ozsváth–Szabó concordance invariant (we describe how to extract this value below). This choice of longitude is illustrated in Figure 3, left. These choices differ by Dehn twists along μ ; note that in both cases $[\mathcal{C}(\gamma)] = [\lambda_0]$ in homology. Different choices of twisting precisely correspond to different unstable chains appearing in [17, Theorem A.11], due to Lipshitz, Ozsváth and Thurston, which Theorem 2 recasts.

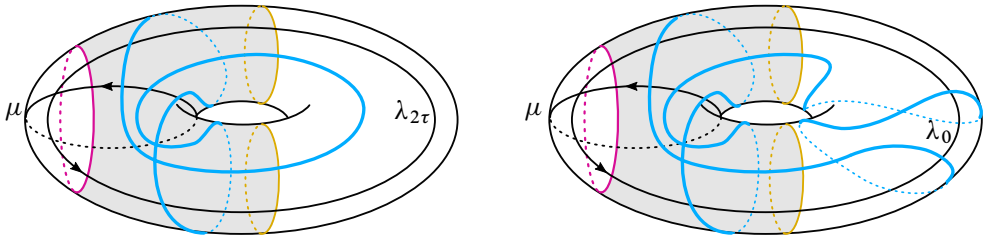


Figure 3: Choices of framing on the right-hand trefoil invariant: $\lambda_{2\tau} = 2\mu + \lambda_0$ (left) and the Seifert longitude λ_0 (right). The resulting curve γ on the boundary of the trefoil exterior coincides with Figure 9 of Hanselman, Rasmussen and Watson [5].

This result generalizes to knots in arbitrary three-manifolds; see Section 5 for further discussion.

A graphical interpretation of the family of concordance homomorphism $\{\phi_i\}$ due to Dai, Hom, Stoffregen and Truong [1] is given by Hanselman and the second author [6]. This can be read off the current picture: Denote by $\gamma_0(K) \subset \gamma(K)$ the noncompact curve in the twice-punctured disk associated with $\mathcal{R}CFK(S^3, K)$. (The curve $\gamma_0(K)$ is a concordance invariant [6, Proposition 2].) Orient $\gamma_0(K)$ so that it leaves from the v -puncture; this is the left-hand puncture in Figure 1, which records the v^i coefficient maps. Contracting the arc a to a point gives a wedge of annuli $A_v \vee A_u$, and the oriented segments of $\gamma_0(K)$ around the v -puncture give a collection of homotopy classes in $\pi_1 A_v \cong \langle t \rangle$, where the generator t winds counterclockwise. As a result, given $\gamma_0(K)$, with our choice of orientation we obtain $t^{n_1} t^{n_2} \dots t^{n_k}$ for the k oriented segments winding around the v -puncture, and

$$\phi_i(K) = \sum_{n_j = \pm i} \text{sign}(n_j), \quad \tau(K) = \sum_{j=1}^k n_j,$$

so that $\tau(K)$ is simply the winding number of γ around the v -puncture. One can check that this gives $\tau(T_{2,3}) = \phi_1(T_{2,3}) = 1$. A more complicated example is shown in Figure 4. The same construction works with the u -puncture instead of the v -puncture, due to a symmetry interchanging u and v in knot Floer homology; see Ozsváth and Szabó [18].

Relevant to concordance is the behaviour under connect sum. Denote by $\mathcal{R}HFK(S^3, K)$ the knot Floer invariant obtained as the homology of a complex $CFK(S^3, K)$ freely generated over \mathcal{R} . In Section 6 we prove:

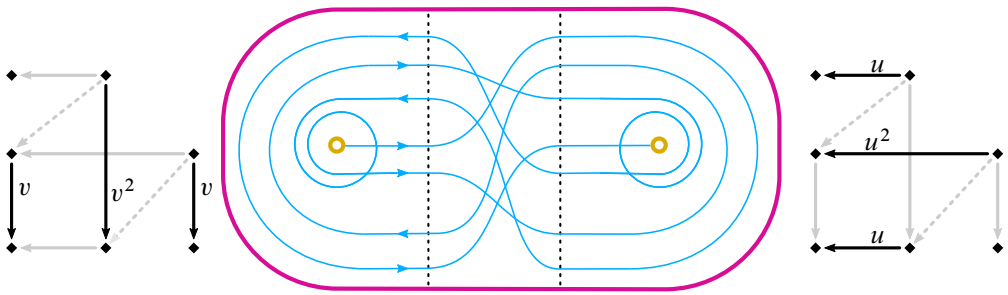


Figure 4: The curve associated with $\mathcal{R}CFK(S^3, K)$ when K is the $(2, 1)$ -cable of the right-hand trefoil. The vertical and horizontal complexes are shown beside the relevant annuli; including the diagonal arrows describes the invariant over $\mathbb{k}[u, v]$. Applying [Theorem 2](#) results in the curve invariant in the torus, which can be compared with [\[6, Figure 1\]](#). Orientating the curve as shown, we calculate $\phi_1(K) = 0$, $\phi_2(K) = 1$ and $\tau(K) = 2$.

Theorem 3 *The knot Floer homology over \mathcal{R} of a connected sum of two knots is equal to the wrapped Lagrangian Floer homology of the corresponding curves:*

$$\mathcal{R}HFK(S^3, mK \# K') \cong HF(\gamma(K), \gamma(K')).$$

A proof is given in [Section 6](#). As is the case with [Theorem 1](#), the proof appeals to the techniques in [\[12, Section 5\]](#).

1 Algebraic objects

Let \mathcal{B} be a bigraded unital algebra over a field \mathbb{k} , with a subring of idempotents \mathcal{I} being equal to \mathbb{k}^n . The object of interest is a bigraded chain complex over \mathcal{B} : Let V be a finite-dimensional bigraded left \mathcal{I} -module, and suppose further that we have a morphism of \mathcal{I} -modules

$$d: V \rightarrow \mathcal{B} \otimes_{\mathcal{I}} V$$

satisfying the compatibility condition

$$(\mu \otimes \text{id}_V) \circ (\text{id}_{\mathcal{B}} \otimes d) \circ d = 0,$$

where μ denotes multiplication in \mathcal{B} . In our setting the morphism d has bidegree $(a, \delta) = (0, 1)$, and the pair (V, d) is a bigraded type D structure over \mathcal{B} .

A couple of remarks: We work with left actions for consistency with [\[17\]](#), and our type D structures will always be reduced, which means that $d(x) = \sum_i b_i \otimes y_i$, where

none of the $b_i \in \mathcal{B}$ are invertible. This is justified by the fact that any bigraded type D structure is homotopy equivalent to a reduced one [12, Lemma 2.16].

Such algebraic structures appear naturally in a variety of settings. For example, given a knot K in S^3 , the knot Floer invariant $HFK(S^3, K)$, due to Ozsváth and Szabó [18] and to Rasmussen [21], can be viewed as a $\mathbb{k}[u, v]$ -module obtained as the homology of a chain complex $CFK(S^3, K)$ over the ring $\mathbb{k}[u, v]$ [22, Section 3]. This complex is freely generated as a module over this ring. As such, it is natural to view $CFK(S^3, K)$ as a type D structure over $\mathbb{k}[u, v]$, which we denote by ${}^{\mathbb{k}[u,v]}CFK(S^3, K)$.

Given a type D structure over \mathcal{B} , a homomorphism of \mathcal{I} -algebras $\mathcal{B} \rightarrow \mathcal{B}'$ gives rise to an induced type D structure over \mathcal{B}' . In particular, the quotient $\mathbb{k}[u, v] \rightarrow \mathbb{k}[u, v]/(uv)$ defines a truncated version of the knot Floer type D structure,

$${}^{\mathcal{R}}CFK(S^3, K) = {}^{\mathbb{k}[u,v]}CFK(S^3, K)|_{uv=0}.$$

The associated module object ${}^{\mathcal{R}}CFK(S^3, K)$ (see [17, Lemma 2.20]) is the knot Floer complex freely generated over \mathcal{R} , which is studied in depth by Dai, Hom, Stoffregen and Truong [1] and Ozsváth and Szabó [19]. A concise formula connecting the type D structure and the associated module object uses the box tensor product (see [16, Section 2.3.2 and Proposition 2.3.18], and also the beginning of Section 4 for a similar construction):

$${}^{\mathcal{R}}CFK(S^3, K) = {}_{\mathcal{R}}\mathcal{R}_{\mathcal{R}} \boxtimes {}^{\mathcal{R}}CFK(S^3, K).$$

We note that there are two further type D structures obtained from ${}^{\mathcal{R}}CFK(S^3, K)$ by setting the appropriate variables equal to zero: the horizontal type D structure C^h and the vertical type D structure C^v . For instance, in the case of the type D structure ${}^{\mathcal{R}}CFK(S^3, T_{2,3})$ (see Figure 2), we have

$$C^h = [\diamond_1 \xleftarrow{u} \diamond_2 \quad \diamond_3], \quad C^v = [\diamond_1 \quad \diamond_2 \xrightarrow{v} \diamond_3].$$

As the type D structures are reduced, the isomorphisms of vector spaces $C^h|_{u=0} \cong \widehat{HFK}(S^3, K) \cong C^v|_{v=0}$ induce an isomorphism

$$\varphi: C^h|_{u=0} \rightarrow C^v|_{v=0}.$$

We have:

Proposition 4 *The data specified by the triple (C^h, C^v, φ) is equivalent to the type D structure ${}^{\mathcal{R}}CFK(S^3, K)$.*

Proof This is immediate from the definitions, but also follows from the discussion in Section 2 outlining the proof of Theorem 1. □

2 Geometric objects

Often, when an invariant of a topological object is a type D structure over an algebra \mathcal{B} , the invariant is only well defined up to homotopy equivalence. As such, it is of general interest to be able to classify homotopy equivalence classes of type D structures. Such classification turns out to be possible when the algebra \mathcal{B} is isomorphic to an endomorphism algebra of certain objects in the (wrapped) Fukaya category of a surface Σ . In this case, homotopy equivalence classes of type D structures over \mathcal{B} correspond to certain curves (decorated with local systems) immersed in Σ . This is a powerful structural result allowing us to translate algebra into geometry, something not so often encountered in mathematics. The classification result is established in [2] using representations of nets; an alternative, more geometric approach is given in [4], which appeals to train tracks in a surface. The simplification algorithm proved in [4] that is central to the classification is further developed and leveraged in [12; 23], where train tracks reappear as precurves. We focus on this latter approach.

To provide a useful toy model for the classification result, we restrict to type D structures over \mathcal{R} . The algebra \mathcal{R} indeed arises as the endomorphism algebra of an object in the (wrapped) Fukaya category of a surface. The surface is the oriented, twice-punctured disk D and the object is an arc connecting the two punctures; see Figure 5. More explicitly, from this figure we can extract a quiver with a single vertex corresponding to the object in the Fukaya category, and arrows labelled u and v corresponding to the two paths around the punctures in D :

$$v \circlearrowleft \diamond \circlearrowright u$$

It is useful to view this quiver as a deformation retract of the twice-punctured disk. The algebra \mathcal{R} is the path algebra of this quiver modulo the relations $uv = 0 = vu$. In terms of Figure 5, these relations have the effect that paths that run along the dashed arc are zero in \mathcal{R} , while paths that only wind around a single puncture are nonzero.

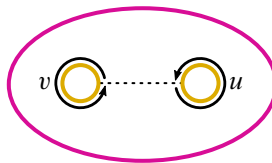


Figure 5: A dual arc system associated with the algebra \mathcal{R} .

To match the setup in [12], a different viewpoint, which is in some sense dual to the previous one, will be more useful. Namely, choose an arc \mathbf{a} that is properly embedded in $(D, \partial D)$ and that divides D into a pair of annuli, as illustrated in Figure 1. From this, we can also recover the quiver: the vertex corresponds to the arc \mathbf{a} and the arrows correspond to paths on the boundary of D . Again, it is useful to consider the quiver as a deformation retract that contracts the arc to the quiver vertex. The relations that we impose on the quiver algebra to obtain \mathcal{R} now have a different geometric interpretation: paths that at an endpoint of the dashed arc continue along the boundary of D are zero in \mathcal{R} , while paths that, at such a point, always choose to follow the dashed arc are nonzero; see also [12, Section 5.1].

The choice of arc \mathbf{a} is an example of an arc system on D , in the sense of Section 5.1 of [12]. In general, an arc system, giving rise to an algebra \mathcal{B} , allows for a graphical representation of type D structures over \mathcal{B} as subobjects of the surface. These show up as train tracks in [4] and precurves in [12]; we describe them explicitly in the case of \mathcal{R} and the twice-punctured disk D . It will be convenient to specify the annuli $D \setminus \mathbf{a} = A_v \sqcup A_u$; these annuli are called faces.

Let (V, d) be a type D structure over \mathcal{R} . Given a homogeneous basis $\{x_1, \dots, x_n\}$ for V (as a vector space over \mathbb{k} , say), we can pick n distinct points on \mathbf{a} and label these with the x_i . To describe the morphism d , suppose $b \otimes x_j$ is a summand of $d(x_i)$. Then, since b is a sum of polynomials, we may assume without loss of generality that b is λu^k or λv^k for some $\lambda \in \mathbb{k}$ and $k > 0$. (The assumption that this power is nonzero comes from our restriction to reduced type D structures.) There are two cases: if $b = \lambda u^k$ then we connect x_i to x_j by an oriented arc immersed in A_u that winds algebraically k times in the positive direction; and if $b = \lambda v^k$ then we connect x_i to x_j by an oriented curve immersed in A_v that winds algebraically k times in the positive direction. In both cases the arc is decorated by the field coefficient λ , noting that when $\lambda = 1$ our convention is to drop the label. In particular, when \mathbb{k} is the two-element field, only the arcs are needed. Lastly, if an intersection point x_i does not have outgoing arcs in the annulus A_u , we connect x_i straight to the u -puncture; we do the same for the A_v annulus and the v -puncture. To see that this information, having added all of the arcs described, can be viewed as an immersed train track in D , we simply require that every curve is perpendicular to \mathbf{a} in a neighbourhood of each x_i . An explicit example is given in Figure 6. Note that in this example there are no arcs going to interior punctures.

These train tracks can be put into a simple form that makes them easier to manage: we require that they are simply faced in the sense of [12, Definition 5.9]. In the present

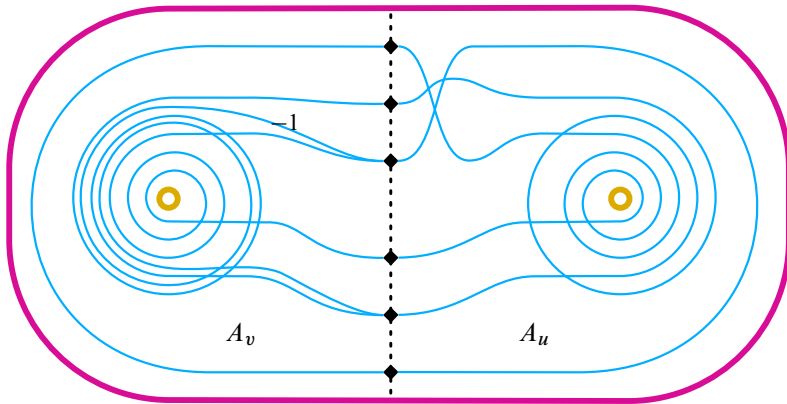


Figure 6: A sample train track representation of a type D structure over \mathcal{R} . Note that every curve segment is oriented so that it runs counterclockwise around a puncture, so this orientation is omitted. Similarly, unlabelled edges (of which there are all but one in this example) carry the decoration $\lambda = 1$.

setting, this amounts to expressing

$$D = A_v \cup_{\mathbf{a} \times \{1\}} (\mathbf{a} \times [-1, 1]) \cup_{\mathbf{a} \times \{-1\}} A_u$$

and requiring that the train track restricted to A_u and to A_v describes a type D structure over $\mathbb{k}[u]$ and $\mathbb{k}[v]$, respectively, with the property that each x_i connects to at most one x_j . For an illustration, see Figure 7. All of the interesting switching is confined to the strip $\mathbf{a} \times [-1, 1]$, which amounts to a graphical interpretation (reading from right to left) of an isomorphism $\varphi: V_u \rightarrow V_v$, where V_v and V_u are the underlying vector spaces associated with the type D structure in each face. As such, the general fact that we can restrict to simply faced train tracks (see [12, Proposition 5.10]) boils down to the fact that type D structures over \mathcal{R} admit vertically and horizontally simplified bases [17, Definition 11.23]—though not necessarily one that is simultaneously vertically and horizontally simplified, whence the choice of isomorphism. This last assertion explains the presence of φ ; compare Proposition 4. We remark that this is one step in which the grading plays a key role.

Aside We make a digression to describe that, in order to classify type D structures in terms of immersed curves, other choices of surface decomposition are possible. Namely, another option would be to

- (1) cut the annuli A_u and A_v further, as described in Figure 8;
- (2) associate with this new geometric picture a different algebra \mathcal{E} ;

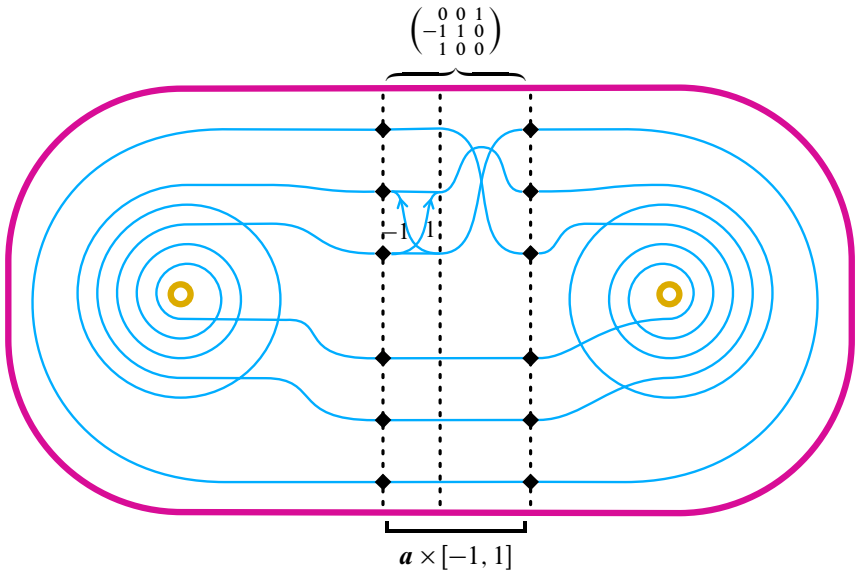


Figure 7: Expressing the train track from Figure 6 as a simply faced precurve. The isomorphism described can be read off the tracks in $a \times [-1, 1]$ from right to left; in the present setting the resulting matrix block-decomposes into two 3×3 parts, of which one is shown and the other is the identity matrix.

- (3) interpret the type D structure $\mathcal{R}V$ as a type D structure $\mathcal{E}W$ over the algebra \mathcal{E} ;
- (4) apply the methods from [4] to interpret $\mathcal{E}W$ as an immersed curve.

To describe this in more detail, let us focus first on the annulus A_v in step (2).

Consider Figure 8. Any type D structure $\mathbb{k}[v]V_\diamond$ may be regarded as a type D structure $V_\bullet \oplus V_\bullet \oplus V_\circ$ over the quiver algebra $\mathbb{k}[\bullet \xrightarrow{a} \diamond \xrightarrow{b} \circ]$ together with an isomorphism between the vector spaces V_\bullet and V_\circ . To repackage the latter into a type D structure without extra data, we consider a subalgebra generated by idempotents $\iota_\bullet + \iota_\circ$ and ι_\diamond .

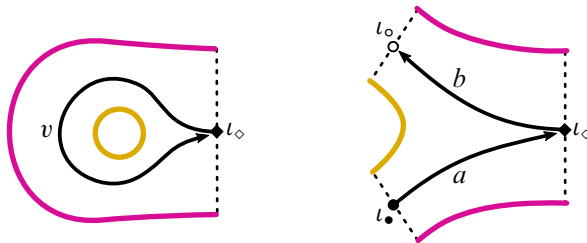


Figure 8: A quiver associated with the annulus describing the algebra $\mathbb{k}[v]$, and a quiver for an algebra associated with an additional cut.

(because eventually the idempotents ι_\circ and ι_\bullet are identified). Writing $\iota_\oplus = \iota_\bullet + \iota_\circ$, the subalgebra is equal to

$$\mathcal{C} = \mathbb{k}[\oplus \begin{array}{c} \xrightarrow{a} \\ \xleftarrow{b} \end{array} \diamond] / (ba).$$

The type D structure ${}^{\mathbb{k}[v]}V_\diamond$ can now be interpreted as a type D structure ${}^{\mathcal{C}}(V_\diamond \oplus V_\oplus)$: generators \diamond in ${}^{\mathbb{k}[v]}V_\diamond$ and ${}^{\mathcal{C}}(V_\diamond \oplus V_\oplus)$ are in one-to-one correspondence, while a differential $\diamond \xrightarrow{v^n} \diamond$ in ${}^{\mathbb{k}[v]}V_\diamond$ corresponds to the sequence of differentials

$$\diamond \xrightarrow{b} \oplus \underbrace{\xrightarrow{ab} \oplus \xrightarrow{ab} \dots \xrightarrow{ab} \oplus}_{n \text{ generators}} \xrightarrow{a} \diamond$$

in ${}^{\mathcal{C}}(V_\diamond \oplus V_\oplus)$. To add the second annulus A_μ to the picture, given a type D structure ${}^{\mathcal{R}}V_\diamond$ one translates it into a type D structure ${}^{\mathcal{E}}W$ over the algebra

$$\mathcal{E} = \mathbb{k}[\oplus_1 \begin{array}{c} \xrightarrow{a_1} \\ \xleftarrow{b_1} \end{array} \diamond \begin{array}{c} \xrightarrow{b_2} \\ \xleftarrow{a_2} \end{array} \oplus_2] / (b_1 a_1, b_2 a_2, a_1 b_2, a_2 b_2)$$

via the dictionary

$$(1) \quad \diamond \xrightarrow{v^n} \diamond \longmapsto \diamond \xrightarrow{b_1} \oplus_1 \underbrace{\xrightarrow{a_1 b_1} \oplus_1 \dots \xrightarrow{a_1 b_1} \oplus_1}_{n \text{ generators}} \xrightarrow{a_1} \diamond,$$

$$(2) \quad \diamond \xrightarrow{u^n} \diamond \longmapsto \diamond \xrightarrow{b_2} \oplus_2 \underbrace{\xrightarrow{a_2 b_2} \oplus_2 \dots \xrightarrow{a_2 b_2} \oplus_2}_{n \text{ generators}} \xrightarrow{a_2} \diamond.$$

With this type D structure ${}^{\mathcal{E}}W$ in hand, the methods from [4] allow us to interpret ${}^{\mathcal{E}}W$ as an immersed curve.

A possible difficulty might arise from the following. The passage from ${}^{\mathcal{R}}V_\diamond$ to ${}^{\mathcal{E}}W$ does not respect homotopy equivalences: there exist homotopy equivalent type D structures ${}^{\mathcal{R}}V_\diamond \simeq {}^{\mathcal{R}}V'_\diamond$ such that the corresponding type D structures ${}^{\mathcal{E}}W$ and ${}^{\mathcal{E}}W'$ are not homotopy equivalent (take for example ${}^{\mathcal{R}}V_\diamond = [\diamond \xleftarrow{v} \diamond \xrightarrow{v} \diamond]$ and ${}^{\mathcal{R}}V'_\diamond = [\diamond \xleftarrow{v} \diamond] \oplus [\diamond]$). This problem is mitigated by the fact that the curves associated with ${}^{\mathcal{E}}W$ and ${}^{\mathcal{E}}W'$ will differ only by how many times their ends wrap around the two punctures, and initially we regard such curves as the same. Another way to mitigate this problem is to find vertically and horizontally simplified bases $\{\xi_i\}$ and $\{\eta_j\}$ for ${}^{\mathcal{R}}V_\diamond$ at the outset, and apply the operation (1) to the basis $\{\xi_i\}$ and the operation (2) to the basis $\{\eta_i\}$. This will ensure that the curve associated with ${}^{\mathcal{E}}W$ will not have extra wrapping around the punctures (and, of course, there may be nontrivial train tracks in the middle as in Figure 7).

We now return to the main text and make some comments about our conventions, reviewing [12, Section 5.6]. The object appearing in the strip $\mathbf{a} \times [-1, 1]$ represents an invertible matrix, where the i^{th} column records the edges leaving the point labelled x_i on $\mathbf{a} \times \{-1\}$ (\mathbf{a} is oriented from top to bottom in our figures, so that $\{-1\}$ is the right-most

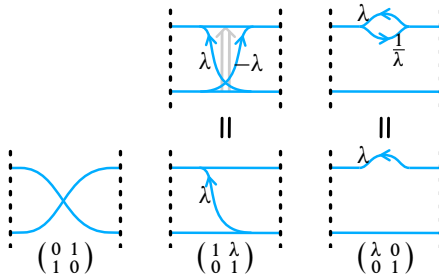


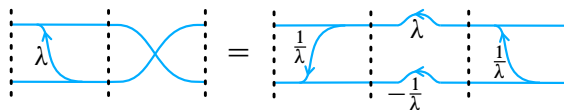
Figure 9: A crossing, a crossover switch, and a passing loop, each with the elementary matrix they represent by reading paths right to left. To declutter pictures, we will be using the pictures in the lower row, where the arrows pointing left to right are dropped.

edge of the strip). Using the row-reduction algorithm, this matrix can be factorized into elementary matrices corresponding to three geometric subobjects, as shown in Figure 9. These subobjects differ from the ones in [4], where the coefficients are restricted to the two-element field. New in the context of general fields are the nonzero coefficients $\lambda \in \mathbb{k}$, recorded on the crossover switches (these correspond to crossover arrows from [4]), as well as the passing loops, which introduce coefficients at various points. The main point is that, when two coefficients appear consecutively on one edge connecting the source and the target, the coefficients multiply, while if two edges share a common source and a common target, the coefficients on those edges add. We note that the geometric objects contain not only the information encoding φ (reading right to left) but also the information about the inverse φ^{-1} (reading left to right). As such, some of the data in the crossover switches and in the passing loops is superfluous. In particular, to simplify pictures here, we will record only the arrows running right to left.

It is convenient to put the matrix representing φ into a normal form, namely the LPU normal form: any invertible matrix can be written as a product of a lower triangular matrix, a permutation matrix (which may be multiplied, additionally, by a diagonal matrix to change coefficients), and an upper triangular matrix. For example, the matrix $\begin{pmatrix} \lambda & 1 \\ 1 & 0 \end{pmatrix}$ may be expressed as

$$\begin{pmatrix} 1 & \lambda \\ 0 & 1 \end{pmatrix} \begin{pmatrix} 0 & 1 \\ 1 & 0 \end{pmatrix} = \begin{pmatrix} 1 & 0 \\ \lambda^{-1} & 1 \end{pmatrix} \begin{pmatrix} \lambda & 0 \\ 0 & -\lambda^{-1} \end{pmatrix} \begin{pmatrix} 1 & \lambda^{-1} \\ 0 & 1 \end{pmatrix}$$

and this identity has the geometric interpretation



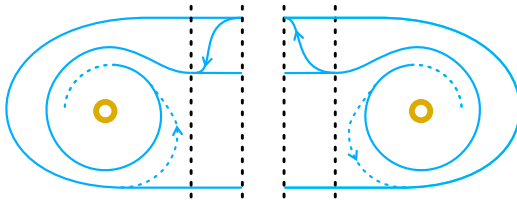


Figure 10: Arrows running counterclockwise can be removed.

More generally, writing the matrix for φ in LPU normal form corresponds to modifying the train track in the region $\mathbf{a} \times [-1, 1]$ so that the downward arrows are on the left, the upward arrows are on the right, and there is a permutation in the middle. A complete list of geometric moves corresponding to different factorizations into elementary matrices is given in [12, Figure 23]. As an example, the reader should compare Figures 7 and 11.

The reason this form is useful is that it allows us to remove arrows and simplify. This is possible in general, by appealing to an algorithm given in [4], and ultimately gives rise to the proof of Theorem 1; see [12, Section 5] for details. The main point is that arrows winding counterclockwise around a puncture can be removed. Namely, suppose there is an arrow near an edge of the strip $\mathbf{a} \times [-1, 1]$ that, when pushed into the relevant annulus, runs counterclockwise between curve segments with different amounts of wrapping. Then there is a homotopy equivalence that produces a new train track — with the counterclockwise arrow removed — representing the same type D structure; see Figure 10. This is described in detail in [12, Lemma 5.11]. The result of this procedure, applied to the example described in Figure 11, is shown in Figure 12.

Recall that a local system over an immersed curve is a vector bundle over the curve. In general, all of our curves carry local systems, but when the associated bundle is one-dimensional and trivial we drop it from the notation. When working with signs, one-dimensional local systems are quite common as the coefficients along any given curve component multiply. Of course, noncompact curves do not carry interesting local systems since all vector bundles are trivial in this case. On the other hand, for compact curves it should be clear from the construction described above where a local system can arise: if two compact curves run parallel, then a crossover switch running between them cannot be removed by a chain isomorphism of type D structures. In general, local systems provide a clean way of presenting the relevant invariants, while the formalism expressing curves with local systems in terms of train tracks gives a concrete means of working with these objects. An example is shown in Figure 13; notice that, by replacing φ with φ^{-1} in this example, one can obtain a vertically simplified basis or

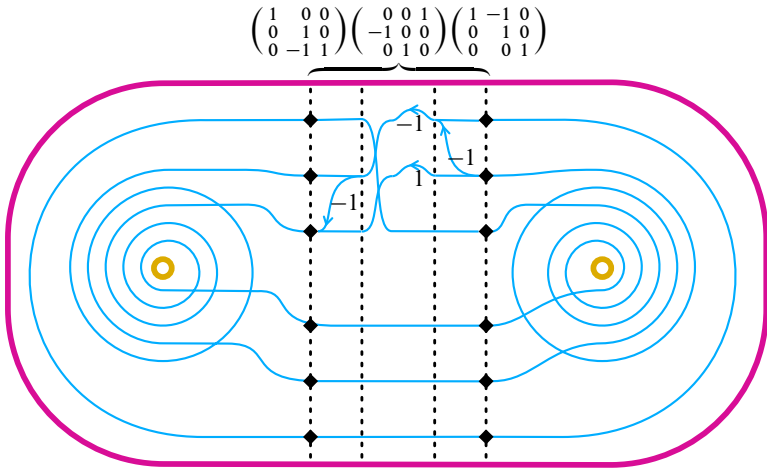


Figure 11: Modifying the train track from Figure 7 according to an LPU decomposition of the matrix.

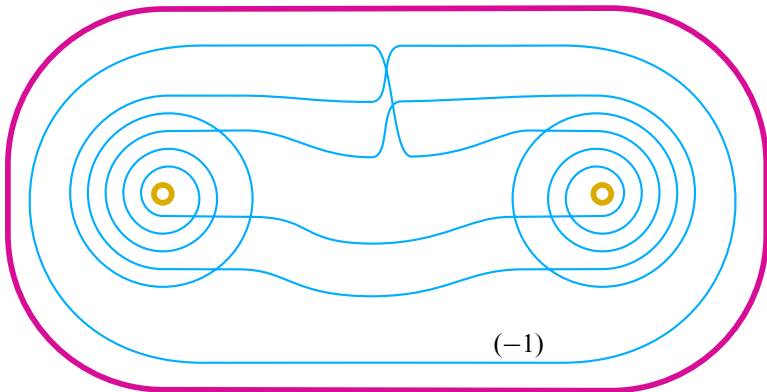


Figure 12: Modifying the train track from Figure 11 by removing the counterclockwise arrows. This produces an immersed curve — an object that is equivalent to the train track from Figure 6, and which carries a one-dimensional local system with automorphism that multiplies by -1 .

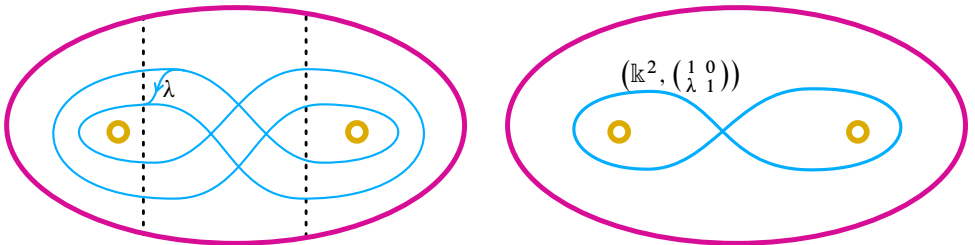
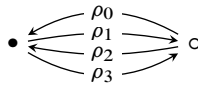


Figure 13: An arrow that cannot be cancelled gives rise to a nontrivial local system.

a horizontally simplified basis, but not both simultaneously. It appears to still be an open question if such phenomena arise for invariants associated with knots; see [11, Remark 2.9].

3 Adding a handle

We now introduce the second algebra: the extended torus algebra $\tilde{\mathcal{A}}$. This algebra is introduced in [4], and is also the algebra arising naturally in our setting. By construction, the map \curvearrowright takes the twice-punctured disk to the once-punctured torus T . An arc system for the latter is shown in Figure 14, from which the associated quiver



can be extracted — as before, we contract the arcs to the quiver vertices. Consulting Figure 16, note that \mathbf{a}_\bullet is identified with the meridian μ and \mathbf{a}_\circ is identified with the choice of longitude λ . With this arc system we associate an algebra $\tilde{\mathcal{A}}$. Analogous to the relation $uv = 0$ from Figure 1, the algebra $\tilde{\mathcal{A}}$ has relations

$$\rho_{i+1}\rho_i = 0$$

(indices interpreted modulo 4), as explained in Section 2. Note that the products $\rho_i\rho_{i+1} = \rho_{i(i+1)}$ are nonzero. For consistency with [4, Section 3.1] we would need to add an additional relation $\rho_0\rho_1\rho_2\rho_3\rho_0 = 0$, but this is not necessary in the present setting.

The arc system associated with $\tilde{\mathcal{A}}$ decomposes the torus into a single disk, so type D structures associated with compact train tracks will be curved. We fix the curvature

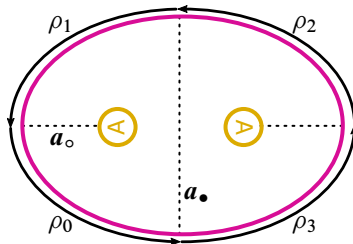


Figure 14: An arc system for the extended algebra $\tilde{\mathcal{A}}$. The two discs are identified, producing a handle.

term $c = \rho_{0123} + \rho_{1230} + \rho_{2301} + \rho_{3012}$. Recall that a curved type D structure over $\tilde{\mathcal{A}}$ satisfies the compatibility condition

$$(\mu \otimes \text{id}_V) \circ (\text{id}_{\tilde{\mathcal{A}}} \otimes d) \circ d = c \cdot \text{id}_{\tilde{\mathcal{A}}}$$

and that, in this setting, the underlying \mathbb{k} -vector space decomposes so that $V = V_\bullet \oplus V_\circ$ as an \mathcal{I} -module.

The torus algebra is the quotient $\mathcal{A} = \tilde{\mathcal{A}}/(\rho_0)$. Notice that in this quotient the curvature vanishes and the compatibility condition for type D structures given in Section 1 is recovered. This algebra is explored in depth in [17, Section 11; 4].

4 The proof of Theorem 2

To set the stage, we first describe three general constructions. First, given a type D structure ${}^{\mathbb{k}[u]}N$ over the polynomial ring $\mathbb{k}[u]$, there is a natural way to produce a dg module/chain complex over $\mathbb{k}[u]$: substitute each generator \diamond in ${}^{\mathbb{k}[u]}N$ with a copy of the ring $\mathbb{k}[u]$, producing a free $\mathbb{k}[u]$ -module, and then endow this module with a differential by substituting every arrow $\diamond \xrightarrow{\ell u^n} \diamond$ in ${}^{\mathbb{k}[u]}N$ with a map $\mathbb{k}[u] \xrightarrow{\cdot(\ell u^n)} \mathbb{k}[u]$ (where $\ell \in \mathbb{k}$). We denote the resulting dg module by $\mathbb{k}[u] \boxtimes {}^{\mathbb{k}[u]}N$, because it coincides with the result of box tensoring the type D structure with the module $\mathbb{k}[u]$ viewed as a bimodule over itself [16, Section 2.3.2]. Note that this operation respects homotopy equivalences and also can be reversed [16, Proposition 2.3.18], albeit in a less than straightforward way.

For the second construction, let $\mathbb{k}[v]$ be the graded polynomial ring in one variable with grading $a(v) = 1$. (Below, a will be the Alexander grading.) Suppose ${}^{\mathbb{k}[v]}N = \bigoplus_{a \in \mathbb{Z}} {}^{\mathbb{k}[v]}N^a$ is a graded type D structure over $\mathbb{k}[v]$ such that the differential preserves the grading a . We can then produce a complex ${}^{\mathbb{k}[v]}N|_{v=1}$ by substituting arrows $\diamond \xrightarrow{\ell v^n} \diamond$ in ${}^{\mathbb{k}[v]}N$ by arrows $\diamond \xrightarrow{\ell} \diamond$. Clearly, this amounts to passing to the quotient $\mathbb{k} = \mathbb{k}[v]/(v - 1)$. However, since $a(v) = 1$, all the differentials in ${}^{\mathbb{k}[v]}N$ that involved v^n for $n \neq 0$ now change the grading in ${}^{\mathbb{k}[v]}N|_{v=1}$ by n . Thus, we can consider ${}^{\mathbb{k}[v]}N|_{v=1}$ as a filtered chain complex, where the filtration levels are $\mathcal{F}_j = \bigoplus_{a \leq j} N^a$. As a category, type D structures over $\mathbb{k}[v]$ are equivalent to filtered chain complexes via the construction above. In particular, type D structure homomorphisms and homotopies between them precisely correspond to filtered chain maps and filtered homotopies between them.

The third construction is similar to the second. Given, a graded type D structure ${}^{\mathbb{k}[v]}N$ over $\mathbb{k}[v]$ whose differential preserves the grading a , we define a complex ${}^{\mathbb{k}[v]}N|_{v=0}$ by removing all arrows $\diamond \xrightarrow{\ell v^n} \diamond$ for $n > 0$ in ${}^{\mathbb{k}[v]}N$. This amounts to passing to the quotient $\mathbb{k} = \mathbb{k}[v]/(v)$ or, equivalently, to passing to the associated graded complex of the filtered complex ${}^{\mathbb{k}[v]}N|_{v=1}$.

We can now provide a dictionary between the knot Floer structures used here and those in [17]. In this paper, the most general knot Floer invariant is the type D structure ${}^{\mathbb{k}[u,v]}CFK(S^3, K)$. In [17], two kinds of invariants appear. The first is the filtered chain complex $CFK^-(S^3, K)$ over $\mathbb{k}[u]$, which is a dg module over $\mathbb{k}[u]$ filtered with respect to the Alexander grading. It is obtained from ${}^{\mathbb{k}[u,v]}CFK(S^3, K)$ by applying the first construction to the variable u and the second construction to the variable v :

$$CFK^-(S^3, K) = \mathbb{k}[u] \boxtimes {}^{\mathbb{k}[u]}({}^{\mathbb{k}[u,v]}CFK(S^3, K)|_{v=1}).$$

The second invariant used in [17] is $gCFK^-(S^3, K)$, the associated graded complex of $CFK^-(S^3, K)$. It is obtained from ${}^{\mathbb{k}[u,v]}CFK(S^3, K)$ by applying the first construction to the variable u and the third construction to the variable v :

$$gCFK^-(S^3, K) = \mathbb{k}[u] \boxtimes {}^{\mathbb{k}[u]}({}^{\mathbb{k}[u,v]}CFK(S^3, K)|_{v=0}).$$

Example Consider the right-hand trefoil and its knot Floer invariants. The type D structure invariant is

$${}^{\mathbb{k}[u,v]}CFK(S^3, T_{2,3}) = [\diamond_1^1 \xleftarrow{u} \diamond_1^0 \xrightarrow{v} \diamond_1^{-1}],$$

where the superscripts and subscripts indicate the Alexander and δ gradings, respectively. Recall that the Alexander and δ gradings are $\text{gr}(u) = (-1, 1)$ and $\text{gr}(v) = (1, 1)$, so that the differential in the type D structure is of bidegree $(a, \delta) = (0, 1)$. The filtered chain complex over $\mathbb{k}[u]$ now becomes

$$CFK^-(S^3, K) = \mathbb{k}[u] \boxtimes {}^{\mathbb{k}[u]}({}^{\mathbb{k}[u,v]}CFK(S^3, K)|_{v=1}) = [\mathbb{k}[u]_1^1 \xleftarrow{u} \mathbb{k}[u]_1^0 \xrightarrow{1} \mathbb{k}[u]_1^{-1}],$$

while the associated graded chain complex over $\mathbb{k}[u]$ is equal to

$$gCFK^-(S^3, K) = \mathbb{k}[u] \boxtimes {}^{\mathbb{k}[u]}({}^{\mathbb{k}[u,v]}CFK(S^3, K)|_{v=0}) = [\mathbb{k}[u]_1^1 \xleftarrow{u} \mathbb{k}[u]_1^0] \oplus [\mathbb{k}[u]_1^{-1}].$$

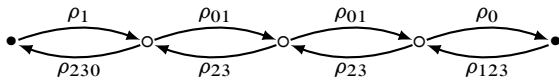
We now proceed to the proof. We start with the knot Floer type D structure

$${}^{\mathcal{R}}CFK(S^3, K) = {}^{\mathbb{F}[u,v]}CFK(S^3, K)|_{vu=0},$$

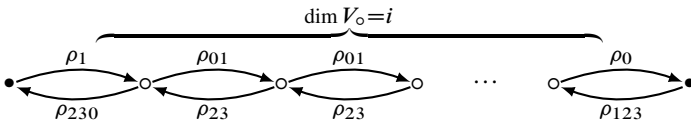
and then homotope it to a representative (following the steps from Section 2) from which the curve invariant γ can be extracted. With the dictionary above in mind,

Theorem A.11 of [17] describes in detail how to pass from $\mathcal{R}CFK(S^3, K)$ to the type D structure ${}^A\widehat{CFD}(M)$, which then produces a curve $\widehat{HF}(M)$ in the punctured torus ∂M . Our task is to prove that the resulting curve coincides with $\mathcal{C}(\gamma)$.

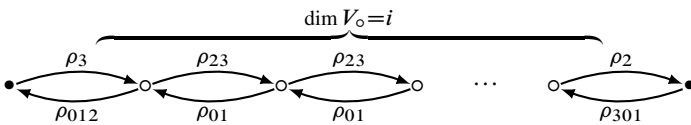
We focus on segments of the curve γ in each of the annuli A_v and A_u , and consider their images under the map \mathcal{C} . Starting with an illustrative example, the image of a curve segment corresponding to the arrow $\diamond \xrightarrow{v^3} \diamond$ is drawn in thick in Figure 15, left, relative to the arc system of the algebra $\tilde{\mathcal{A}}$. Focussing on the first part of this segment, shown are the two ways in can be retracted to the boundary of the torus union the two arcs: in one case the homotoped path runs along ρ_1 , and in the other case it runs along ρ_2 then ρ_3 then ρ_0 . In the type D structure language, then, according to [4] and the discussion in Section 2, this part of the curve results in $\bullet \leftarrow_{\rho_{230}}^{\rho_1} \circ$. Similarly, the whole thick curve segment depicted in Figure 15, left, corresponds to the following part of a type D structure over $\tilde{\mathcal{A}}$:



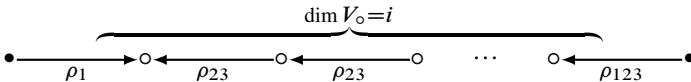
More generally, the image of a curve segment corresponding to the arrow $\diamond \xrightarrow{v^i} \diamond$ is



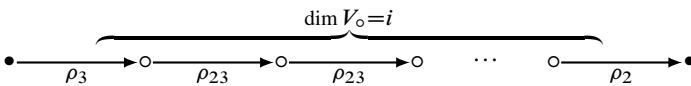
Analogously, the image of a curve segment corresponding to the arrow $\diamond \xrightarrow{u^i} \diamond$ is



Passing to the quotient algebra \mathcal{A} by setting $\rho_0 = 0$ simplifies the above two images to



and



These are precisely the two *stable* chains appearing in the statement of Theorem A.11 of [17]; according to their result, these are the parts of ${}^A\widehat{CFD}(M)$ that correspond to the differentials $\diamond \xrightarrow{v^i} \diamond$ and $\diamond \xrightarrow{u^i} \diamond$ in $\mathcal{R}CFK(S^3, K)$.

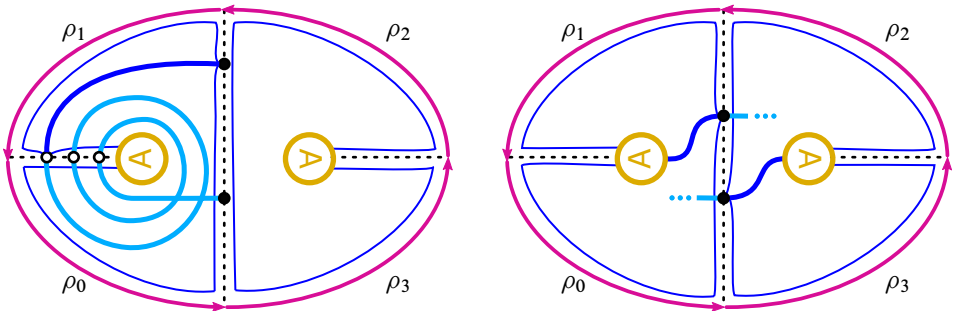


Figure 15: Sample parts of the curve corresponding to a stable chain (left) and an unstable chain (right) from [17, Theorem A.11].

The main subtlety is the appearance of the *unstable* chain, which we have already touched on. Defining \curvearrowright in such a way that there is no extra twisting introduced (see Figure 3, left), the straight segment running over the handle in Figure 15, right, retracts in the two ways shown, producing the final part of the type D structure, $\bullet \xleftarrow{\rho_{12}} \bullet$. Setting $\rho_0 = 0$ results in $\bullet \xrightarrow{\rho_{12}} \bullet$, which is precisely the unstable chain from [17, Theorem A.11]; according to their result, this is the final piece (in addition to the stable chains) in ${}^A\widehat{CFD}(M)$ (computed relative to the parametrization $(\mu, 2\tau)$ of the torus $T^2 = \partial M$). In [17, Theorem A.11], this final piece connects the distinguished generators ξ_0 and η_0 in the vertically and horizontally simplified bases of $CFK^-(K)$. It is left to note that the two generators in Figure 15, right, are precisely ξ_0 and η_0 , because each is incident to only one arrow $\xrightarrow{v^i}$ or $\xrightarrow{u^j}$ in the complex ${}^{\mathcal{R}}CFK(S^3, K)$. We also remark that, while the unstable chain $\bullet \xrightarrow{\rho_{12}} \bullet$ corresponds to the 2τ -framing of the knot K , there are other type D structure presentations of the unstable chain in [17, Theorem A.11], and those would correspond to other choices of twisting in \curvearrowright .

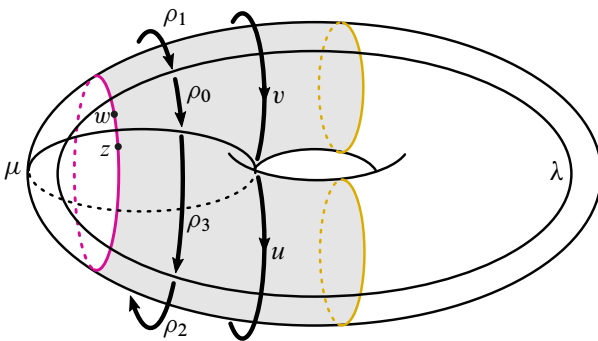


Figure 16: Both algebras \mathcal{R} and $\tilde{\mathcal{A}}$ in context.

The statement about the reverse operation follows from the discussion above. Namely, its clear that $\mathfrak{S} \circ \mathfrak{S}(\widehat{\smile}(\boldsymbol{\gamma})) = \boldsymbol{\gamma}$, and, since we proved $\widehat{\smile}(\boldsymbol{\gamma}) = \widehat{HF}(M)$, we obtain $\mathfrak{S} \circ \mathfrak{S}(\widehat{HF}(M)) = \boldsymbol{\gamma}$.

5 Comments on generalizations and related work

Perhaps the most interesting step in this constructive review of the Lipshitz–Ozsváth–Thurston correspondence comes about when the endpoints of the noncompact component $\boldsymbol{\gamma}_0 \subset \boldsymbol{\gamma}$ are identified to give a new compact component in the once-punctured torus. Note that the output of $\widehat{\smile}$ is always a compact curve, and this is consistent with the observation that $\widehat{HF}(M)$ is a compact curve. The latter, in turn, follows from the fact that $\widehat{CFD}(M)$ is an extendable type D structure [4, Appendix].

Joining the endpoints of the immersed curve $\boldsymbol{\gamma}_0$ associated with a knot K requires a choice of automorphism of \mathbb{k}^n where n is the number of components in $\boldsymbol{\gamma}_0$. Denote the horizontal homology by $H^h = H_*(C^h|_{u=1})$ and the vertical homology by $H^v = H_*(C^v|_{v=1})$. Then, in Theorem 2, because the knot is in S^3 , it follows that $n = 1$ and the automorphism is given, tautologically, by

$$H^v(CFK^-(S^3, K)) \cong H^h(CFK^-(S^3, K)) \cong \widehat{HF}(S^3) \cong \mathbb{k},$$

as explained in [17, Section 11.5]. Thus, the operation $\widehat{\smile}$ is defined over any field provided that we choose a coefficient $a \in \mathbb{k}$ when we identify the ends of $\boldsymbol{\gamma}_0$ along a handle. We choose this coefficient to be $+1$ so that the bordered invariant for the solid torus is a circle with the trivial local system. We note that bordered Floer homology is only defined over the two-element field \mathbb{F} . As such, the map $\widehat{\smile}$ and Theorem 2 gives a *candidate* bordered invariant for the knot exterior when $\mathbb{k} \neq \mathbb{F}$.

We now consider the general case of a knot K in Y . Decomposing along spin^c -structures, the same strategy as above works if Y is an L -space [8]. More generally, however, one needs to know the isomorphism

$$H^v(CFK^-(Y, K)) \cong H^h(CFK^-(Y, K)) \cong \widehat{HF}(Y)$$

(which may be block-decomposed according to spin^c -structures). This recovers a generalization of [17, Theorem A.11], which may be found in forthcoming work of Hockenhull [9] building on his invariant $\text{Poly}(L, \Lambda)$ [10]. From our perspective, the passage from the knot Floer homology of a knot K in Y to the bordered invariants of $Y \setminus \mathring{\nu}(K)$ requires the isomorphism shown above. As there is a decomposition

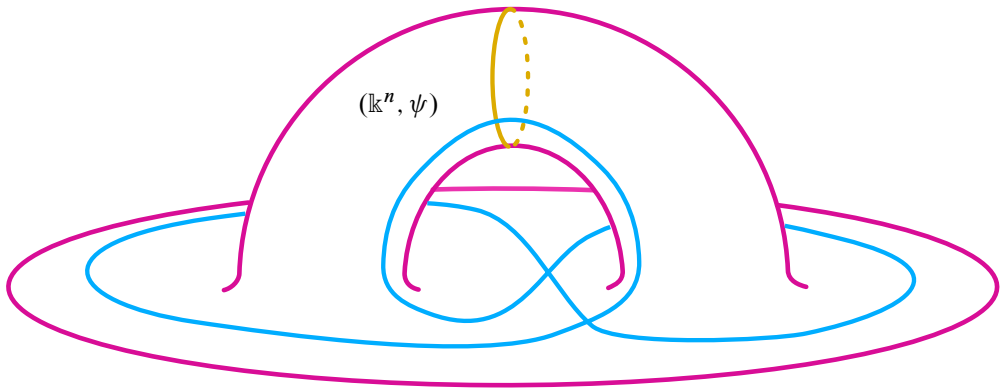


Figure 17: A sample hypothetical local system, where $n = \dim \widehat{HF}(Y)$.

according to spin^c -structures, there is no loss of generality in considering the case where Y is an integer homology sphere. When such a Y is not an L -space, we have that $\dim \widehat{HF}(Y) > 1$ and, in principle, the automorphism ψ induced by the isomorphism between the homologies H^h and H^v can be interesting. In particular, while all components of $\gamma_0(K)$ carry trivial local systems, the new compact object $\widehat{\mathcal{C}}(\gamma_0(K))$ obtains an additional local system (\mathbb{k}^n, ψ) ; see Figure 17. The key point of difference is that the output will be equivalent to a simply faced precurve (in the torus) in general, and a further application of the arrow sliding algorithm may be required to obtain immersed curves. The algebraic side of this story is laid out carefully by Hockenhull [9; 10].

Finally, Hanselman gives another approach [3]: his construction takes the complex $CFK^-(K)$ and outputs an immersed curve in the strip covering the twice-punctured disk D , containing a countable set of pairs of punctures. This cover of the disk is useful for recording the Alexander grading, and also works with general fields (hence producing candidate bordered invariants). We advertise that Hanselman’s construction has a different aim in mind, namely a candidate bordered-minus invariant obtained by promoting the curves to describe type D structures over $\mathbb{k}[u, v]$.

6 The proof of Theorem 3

For simplicity we first focus on the case of the two-element field $\mathbb{k} = \mathbb{F}$. A few properties of the invariant $\mathcal{R}CFK(S^3, K)$ are needed for the proof. First, given two type D structures over the polynomial algebra $\mathbb{k}[u, v]$ or its quotient \mathcal{R} , their tensor

product is another type D structure

$$(V, d) \otimes (V', d') = (V \otimes_{\mathbb{k}} V', d \otimes \text{id} + \text{id} \otimes d').$$

Now, reformulating [18, Theorem 7.1], the behaviour of knot Floer homology under taking the connected sum can be described as

$$\mathcal{R}CFK(S^3, K \# K') \simeq \mathcal{R}(\mathcal{R}CFK(S^3, K) \otimes \mathcal{R}CFK(S^3, K')).$$

The mirroring operation is also well understood — see [18, Proposition 3.7] —

$$\mathcal{R}CFK(S^3, mK) \simeq \mathcal{R}\overline{CFK(S^3, K)},$$

where the latter is the *dual type D structure*, equal to the original one but with all differentials reversed [15, Definition 2.5] (since \mathcal{R} is commutative, the fact that dualizing turns left type D structure to right ones is not a problem). Finally, we need an algebraic relationship between morphism spaces of type D structures [16, Section 2.2.3] and their tensor products. Given any two type D structures, the definitions imply the isomorphism of chain complexes

$$\mathcal{R} \boxtimes \mathcal{R}(\mathcal{R}\overline{N} \otimes \mathcal{R}N') \cong \text{Mor}(\mathcal{R}N, \mathcal{R}N').$$

With the properties above in place, the proof of Theorem 3 is the sequence of isomorphisms

$$\begin{aligned} \mathcal{R}HFK(S^3, mK \# K') &\cong H_*(\mathcal{R} \boxtimes \mathcal{R}CFK(S^3, mK \# K')) \\ &\cong H_*(\mathcal{R} \boxtimes \mathcal{R}[\mathcal{R}CFK(S^3, mK) \otimes \mathcal{R}CFK(S^3, K')]) \\ &\cong H_*(\mathcal{R} \boxtimes \mathcal{R}[\mathcal{R}\overline{CFK(S^3, K)} \otimes \mathcal{R}CFK(S^3, K')]) \\ &\cong H_*(\text{Mor}(\mathcal{R}CFK(S^3, K), \mathcal{R}CFK(S^3, K'))) \\ &\cong HF(\boldsymbol{\gamma}(K), \boldsymbol{\gamma}(K')), \end{aligned}$$

where the final isomorphism follows from the general description of morphism spaces between type D structures over surface algebras [12, Theorem 1.5].

The recipe for adding signs follows the Koszul sign rule, which is discussed in Section 12 of [20] in detail. We find that the resulting signs are a bit more natural if one considers right type D structures [12, Example 2.10], rather than left ones [20, Section 12.3], as then there are no extra signs when box tensoring with $-\boxtimes_{\mathcal{R}}\mathcal{R}$; this is explained in [12, page 19]. Now, since the algebra \mathcal{R} is commutative, our left type D structures can be viewed as right type D structures, and after that filling in the signs becomes straightforward. We refer the reader to [12, Sections 2 and 5]. □

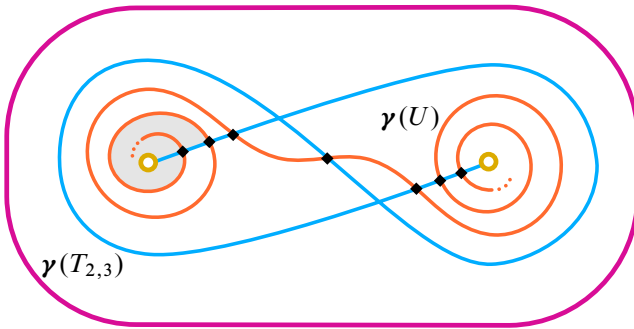


Figure 18: Illustrating [Theorem 3](#) in the case of the unknot $K = U$ and the right-hand trefoil $K' = T_{2,3}$. The curve $\gamma(U)$ is a horizontal arc connecting the punctures, but because we are in the wrapped setting, one needs to wrap $\gamma(U)$ infinitely many times around the punctures when pairing with another curve.

To illustrate this gluing result, suppose $K = U$ and $K' = T_{2,3}$. Then the knot Floer homology of the connected sum is equal to

$$\begin{aligned} \mathcal{R}HF\mathcal{K}(S^3, T_{2,3}) &= H_*(\mathcal{R} \xleftarrow{v} \mathcal{R} \xrightarrow{u} \mathcal{R}) \\ &= [\dots \xleftarrow{v} \diamond \xleftarrow{v} \diamond \xleftarrow{v} \diamond \xrightarrow{u} \diamond \xleftarrow{v} \diamond \xrightarrow{u} \diamond \xrightarrow{u} \diamond \xrightarrow{u} \diamond \dots], \end{aligned}$$

where the arrows indicate the \mathcal{R} -action. The corresponding wrapped Lagrangian Floer homology $HF(\gamma(U), \gamma(T_{2,3}))$ is illustrated in [Figure 18](#). Note that in this example the \mathcal{R} -action can be seen geometrically by counting Maslov index 2 disks covering the punctures; one of these is shaded in the picture. The same is true for the $\mathbb{k}[H]$ -action on Bar-Natan homology, viewed as wrapped Lagrangian Floer homology of immersed curves in [\[12, Example 7.7\]](#). In general, to recover these module-structures, only some of the Maslov index 2 disks should be counted — we will investigate this in future work.

Acknowledgements

This short paper benefited from stimulating conversations with Jonathan Hanselman, Thomas Hockenhull and Matthew Stoffregen. The work was initiated during the CRM50 thematic program *Low-dimensional topology* and we thank the CRM and CIRGET for hosting a great event.

Kotelskiy is supported by an AMS–Simons travel grant. Watson is supported by an NSERC discovery/accelerator grant and was partially supported by funding from the Simons Foundation and the Centre de Recherches Mathématiques, through the

Simons–CRM scholar-in-residence program. Zibrowius is supported by the Emmy Noether Programme of the DFG, project number 412851057, and the SFB 1085 *Higher invariants* in Regensburg.

References

- [1] **I Dai, J Hom, M Stoffregen, L Truong**, *More concordance homomorphisms from knot Floer homology*, *Geom. Topol.* 25 (2021) 275–338 [MR](#) [Zbl](#)
- [2] **F Haiden, L Katzarkov, M Kontsevich**, *Flat surfaces and stability structures*, *Publ. Math. Inst. Hautes Études Sci.* 126 (2017) 247–318 [MR](#) [Zbl](#)
- [3] **J Hanselman**, *Knot Floer homology as immersed curves*, preprint (2023) [arXiv 2305.16271](#)
- [4] **J Hanselman, J Rasmussen, L Watson**, *Bordered Floer homology for manifolds with torus boundary via immersed curves*, preprint (2016) [arXiv 1604.03466](#) To appear in *J. Amer. Math. Soc.*
- [5] **J Hanselman, J Rasmussen, L Watson**, *Heegaard Floer homology for manifolds with torus boundary: properties and examples*, *Proc. Lond. Math. Soc.* 125 (2022) 879–967 [MR](#)
- [6] **J Hanselman, L Watson**, *Cabling in terms of immersed curves*, *Geom. Topol.* 27 (2023) 925–952 [MR](#) [Zbl](#)
- [7] **M Hedden, C M Herald, P Kirk**, *The pillowcase and perturbations of traceless representations of knot groups*, *Geom. Topol.* 18 (2014) 211–287 [MR](#) [Zbl](#)
- [8] **M Hedden, A S Levine**, *Splicing knot complements and bordered Floer homology*, *J. Reine Angew. Math.* 720 (2016) 129–154 [MR](#) [Zbl](#)
- [9] **T Hockenhull**, *Duality patterns in knot Floer homology*, in preparation
- [10] **T Hockenhull**, *Holomorphic polygons and the bordered Heegaard Floer homology of link complements*, preprint (2018) [arXiv 1802.02443](#)
- [11] **J Hom**, *Heegaard Floer invariants and cabling*, PhD thesis, University of Pennsylvania (2011) Available at <https://repository.upenn.edu/edissertations/329/>
- [12] **A Kotelskiy, L Watson, C Zibrowius**, *Immersed curves in Khovanov homology*, preprint (2019) [arXiv 1910.14584](#)
- [13] **Y Lekili, A Polishchuk**, *Auslander orders over nodal stacky curves and partially wrapped Fukaya categories*, *J. Topol.* 11 (2018) 615–644 [MR](#) [Zbl](#)
- [14] **Y Lekili, A Polishchuk**, *Homological mirror symmetry for higher-dimensional pairs of pants*, *Compos. Math.* 156 (2020) 1310–1347 [MR](#) [Zbl](#)
- [15] **R Lipshitz, P S Ozsváth, D P Thurston**, *Heegaard Floer homology as morphism spaces*, *Quantum Topol.* 2 (2011) 381–449 [MR](#) [Zbl](#)

- [16] **R Lipshitz, P S Ozsváth, D P Thurston**, *Bimodules in bordered Heegaard Floer homology*, *Geom. Topol.* 19 (2015) 525–724 [MR](#) [Zbl](#)
- [17] **R Lipshitz, P S Ozsvath, D P Thurston**, *Bordered Heegaard Floer homology*, *Mem. Amer. Math. Soc.* 1216, Amer. Math. Soc., Providence, RI (2018) [MR](#) [Zbl](#)
- [18] **P Ozsváth, Z Szabó**, *Holomorphic disks and knot invariants*, *Adv. Math.* 186 (2004) 58–116 [MR](#) [Zbl](#)
- [19] **P Ozsváth, Z Szabó**, *Algebras with matchings and knot Floer homology*, preprint (2019) [arXiv 1912.01657](#)
- [20] **P Ozsváth, Z Szabó**, *Bordered knot algebras with matchings*, *Quantum Topol.* 10 (2019) 481–592 [MR](#) [Zbl](#)
- [21] **J A Rasmussen**, *Floer homology and knot complements*, PhD thesis, Harvard University (2003) [MR](#) [arXiv math/0306378](#)
- [22] **I Zemke**, *Connected sums and involutive knot Floer homology*, *Proc. Lond. Math. Soc.* 119 (2019) 214–265 [MR](#) [Zbl](#)
- [23] **C Zibrowius**, *Peculiar modules for 4-ended tangles*, *J. Topol.* 13 (2020) 77–158 [MR](#) [Zbl](#)

*Department of Mathematics, Indiana University
Bloomington, IN, United States*

*Current address: Department of Mathematics, Stony Brook University
Stony Brook, NY, United States*

*Department of Mathematics, University of British Columbia
Vancouver, BC, Canada*

*Faculty of Mathematics, University of Regensburg
Regensburg, Germany*

*Current address: Department of Mathematical Sciences, Durham University
Durham, United Kingdom*

artofkot@gmail.com, liam@math.ubc.ca, claudius.zibrowius@posteo.net

<https://artofkot.github.io/>, <https://personal.math.ubc.ca/~liam/>,
<https://cbz20.raspberrypi.com/>

Received: 30 July 2020 Revised: 8 October 2021

ALGEBRAIC & GEOMETRIC TOPOLOGY

msp.org/agt

EDITORS

PRINCIPAL ACADEMIC EDITORS

John Etnyre
etnyre@math.gatech.edu
Georgia Institute of Technology

Kathryn Hess
kathryn.hess@epfl.ch
École Polytechnique Fédérale de Lausanne

BOARD OF EDITORS

Julie Bergner	University of Virginia jeb2md@eservices.virginia.edu	Robert Lipshitz	University of Oregon lipshitz@uoregon.edu
Steven Boyer	Université du Québec à Montréal cohf@math.rochester.edu	Norihiko Minami	Nagoya Institute of Technology nori@nitech.ac.jp
Tara E. Brendle	University of Glasgow tara.brendle@glasgow.ac.uk	Andrés Navas	Universidad de Santiago de Chile andres.navas@usach.cl
Indira Chatterji	CNRS & Université Côte d'Azur (Nice) indira.chatterji@math.cnrs.fr	Thomas Nikolaus	University of Münster nikolaus@uni-muenster.de
Alexander Dranishnikov	University of Florida dranish@math.ufl.edu	Robert Oliver	Université Paris 13 bobol@math.univ-paris13.fr
Corneli Druţu	University of Oxford cornelia.drutu@maths.ox.ac.uk	Birgit Richter	Universität Hamburg birgit.richter@uni-hamburg.de
Tobias Ekholm	Uppsala University, Sweden tobias.ekholm@math.uu.se	Jérôme Scherer	École Polytech. Féd. de Lausanne jerome.scherer@epfl.ch
Mario Eudave-Muñoz	Univ. Nacional Autónoma de México mario@matem.unam.mx	Zoltán Szabó	Princeton University szabo@math.princeton.edu
David Futер	Temple University dfuter@temple.edu	Ulrike Tillmann	Oxford University tillmann@maths.ox.ac.uk
John Greenlees	University of Warwick john.greenlees@warwick.ac.uk	Maggy Tomova	University of Iowa maggy-tomova@uiowa.edu
Ian Hambleton	McMaster University ian@math.mcmaster.ca	Nathalie Wahl	University of Copenhagen wahl@math.ku.dk
Hans-Werner Henn	Université Louis Pasteur henn@math.u-strasbg.fr	Chris Wendl	Humboldt-Universität zu Berlin wendl@math.hu-berlin.de
Daniel Isaksen	Wayne State University isaksen@math.wayne.edu	Daniel T. Wise	McGill University, Canada daniel.wise@mcgill.ca
Christine Lescop	Université Joseph Fourier lescop@ujf-grenoble.fr		


See inside back cover or msp.org/agt for submission instructions.

The subscription price for 2023 is US \$650/year for the electronic version, and \$940/year (+ \$70, if shipping outside the US) for print and electronic. Subscriptions, requests for back issues and changes of subscriber address should be sent to MSP. Algebraic & Geometric Topology is indexed by [Mathematical Reviews](#), [Zentralblatt MATH](#), [Current Mathematical Publications](#) and the [Science Citation Index](#).

Algebraic & Geometric Topology (ISSN 1472-2747 printed, 1472-2739 electronic) is published 9 times per year and continuously online, by Mathematical Sciences Publishers, c/o Department of Mathematics, University of California, 798 Evans Hall #3840, Berkeley, CA 94720-3840. Periodical rate postage paid at Oakland, CA 94615-9651, and additional mailing offices. POSTMASTER: send address changes to Mathematical Sciences Publishers, c/o Department of Mathematics, University of California, 798 Evans Hall #3840, Berkeley, CA 94720-3840.

AGT peer review and production are managed by EditFlow[®] from MSP.

PUBLISHED BY

 **mathematical sciences publishers**
nonprofit scientific publishing

<http://msp.org/>

© 2023 Mathematical Sciences Publishers

ALGEBRAIC & GEOMETRIC TOPOLOGY

Volume 23

Issue 6 (pages 2415–2924)

2023

An algorithmic definition of Gabai width	2415
RICKY LEE	
Classification of torus bundles that bound rational homology circles	2449
JONATHAN SIMONE	
A mnemonic for the Lipshitz–Ozsváth–Thurston correspondence	2519
ARTEM KOTELSKIY, LIAM WATSON and CLAUDIUS ZIBROWIUS	
New bounds on maximal linkless graphs	2545
RAMIN NAIMI, ANDREI PAVELESCU and ELENA PAVELESCU	
Legendrian large cables and new phenomenon for nonuniformly thick knots	2561
ANDREW MCCULLOUGH	
Homology of configuration spaces of hard squares in a rectangle	2593
HANNAH ALPERT, ULRICH BAUER, MATTHEW KAHLE, ROBERT MACPHERSON and KELLY SPENDLOVE	
Nonorientable link cobordisms and torsion order in Floer homologies	2627
SHERRY GONG and MARCO MARENGON	
A uniqueness theorem for transitive Anosov flows obtained by gluing hyperbolic plugs	2673
FRANÇOIS BÉGUIN and BIN YU	
Ribbon 2–knot groups of Coxeter type	2715
JENS HARLANDER and STEPHAN ROSEBROCK	
Weave-realizability for D –type	2735
JAMES HUGHES	
Mapping class groups of surfaces with noncompact boundary components	2777
RYAN DICKMANN	
Pseudo-Anosov homeomorphisms of punctured nonorientable surfaces with small stretch factor	2823
SAYANTAN KHAN, CALEB PARTIN and REBECCA R WINARSKI	
Infinitely many arithmetic alternating links	2857
MARK D BAKER and ALAN W REID	
Unchaining surgery, branched covers, and pencils on elliptic surfaces	2867
TERRY FULLER	
Bifiltrations and persistence paths for 2–Morse functions	2895
RYAN BUDNEY and TOMASZ KACZYNSKI	